Regulation of Desmosome Assembly in Epithelial Cells: Kinetics of Synthesis, Transport, and Stabilization of Desmoglein I, a Major Protein of the Membrane Core Domain

Manijeh Pasdar and W. James Nelson

Institute for Cancer Research, Philadelphia, Pennsylvania 19111

Abstract. Desmosomes are composed of two morphologically and biochemically distinct domains, a cytoplasmic plaque and membrane core. We have initiated a study of the synthesis and assembly of these domains in Madin-Darby canine kidney (MDCK) epithelial cells to understand the mechanisms involved in the formation of desmosomes. Previously, we reported the kinetics of assembly of two components of the cytoplasmic plaque domain, Desmoplakin I/II (Pasdar, M., and W. J. Nelson. 1988. *J. Cell Biol.* 106:677–685 and 106:687–699. We have now extended this analysis to include a major glycoprotein component of the membrane core domain, Desmoglein I (DGI; M_r = 150,000). Using metabolic labeling and inhibitors of glycoprotein processing and intracellular transport, we show that DGI biosynthesis is a sequential process with defined stages. In the absence of cell–cell contact, DGI enters a Triton X-100 soluble pool and is core glycosylated. The soluble DGI is then transported to the Golgi complex where it is first complex glycosylated and then titrated into an insoluble pool. The insoluble pool of DGI is subsequently transported to the plasma membrane and is degraded rapidly ($t_{½}$ < 4 h). Although this biosynthetic pathway occurs independently of cell–cell contact, induction of cell–cell contact results in dramatic increases in the efficiency and rate of titration of DGI from the soluble to the insoluble pool, and its transport to the plasma membrane where DGI becomes metabolically stable ($t_{½}$ > 24 h). Taken together with our previous study of DPI/II, we conclude that newly synthesized components of the cytoplasmic plaque and membrane core domains are processed and assembled with different kinetics indicating that, at least initially, each domain is assembled separately in the cell. However, upon induction of cell–cell contact there is a rapid titration of both components into an insoluble and metabolically stable pool at the plasma membrane that is concurrent with desmosome assembly.

DESMOSOMES are major components of the intercellular junctional complex of epithelia. They form on the plasma membrane of adjacent cells upon induction of cell–cell contact, and play important roles in cell adhesion and in maintaining the structural and functional interaction of adjacent cells (6, 10, 14, 15, 20, 21, 34). Detailed morphological and biochemical studies have shown that desmosomes consist of several proteins organized into two structurally and functionally distinct domains, a cytoplasmic plaque and membrane core (2–5, 7, 8, 10, 16, 22, 47). Morphologically, the cytoplasmic plaque appears as a discrete electron-dense plaque beneath the plasma membrane (4, 13, 16, 26). Biochemically, the plaque is composed of nonglycosylated proteins (the desmoplakins [DP]) with apparent relative molecular masses of 250,000 (DPI), 215,000 (DPII), 83,000 (DPIII also called Plakoglobin), and 78,000 (DPIV) (3, 7, 8, 12, 13, 22, 27, 45). The cytoplasmic plaque is the binding site for cytokeratin intermediate filaments and is localized subjacent to the membrane core domain (6, 10, 32, 36). Biochemically, the membrane core domain is composed of glycoproteins (the desmogleins [DG]) with apparent relative molecular masses of 150,000 (DGI), 120,000/110,000 (DGII/DGIII), and 22,000 (DGIV)(2, 3, 5, 22, 26, 44, 45). The membrane core domain is thought to be involved in the adhesive function of the desmosome (5, 6, 15, 34).

Early morphological studies demonstrated that desmosomes are assembled rapidly on the plasma membranes of adjacent epithelial cells upon induction of cell–cell contact (20, 21, 32–36). Furthermore, assembly occurs from preexisting pools of proteins in the cytoplasm and on the plasma membrane (5, 14, 24, 38, 39). However, the mechanisms that regulate the biosynthesis of the two domains and their assembly into a desmosome upon cell–cell contact are unknown. To address this question we have initiated a study of the regulation of assembly of desmosomes in Madin-Darby canine

1. *Abbreviations used in this paper*: CSK, cytoskeleton extraction; DG, desmoglein; DP, desmoplakin; endoH, endo-β-*N*-acetylglucosaminidase; HCM, high (1.8 mM) Ca^{++}-containing medium; LCM, low (5 μM) Ca^{++}-containing medium.

kidney (MDCK) epithelial cells by analyzing the kinetics of synthesis, stabilization, and assembly of individual components of the cytoplasmic plaque and membrane core domains.

Previously, we reported the results of the first detailed analysis of the assembly of two major components of the cytoplasmic plaque domain, desmoplakins I and II (DPI/II) (38, 39). Our biochemical and morphological analyses showed that the assembly of DPI/II into desmosomes comprises at least three stages. Stage I involves the formation of a soluble ~7.3-S complex of newly synthesized DPI/II in a 3:1 molar ratio. This soluble complex appears to be associated with cytokeratin intermediate filaments but can be easily extracted from the cell in a buffer containing high salt and Triton X-100 (cytoskeleton extraction buffer [CSK]). Stage II involves the titration of ~30% of DPI/II from the soluble pool into an insoluble pool that appears to be tightly bound to cytokeratins and is not extractable from the cell with CSK buffer. Stages I and II occur independently of cell-cell contact, but in the absence of cell-cell contact both protein pools are metabolically unstable ($t_{½}$ = 8–10 h). Stage III requires cell-cell contact. Upon induction of cell-cell contact the capacity of the insoluble pool gradually increases threefold (within 3–5 h) and ~75% of DPI/II are titrated from the soluble pool into the insoluble pool. Subsequently, the insoluble pool of DPI/II moves to the plasma membrane and becomes stabilized as part of assembled desmosomes ($t_{½}$ > 72 h). DPI/II that remain in the soluble pool are less stable ($t_{½}$ < 8–10 h).

To understand the mechanisms that regulate assembly of both desmosomal domains into a single structure we have now extended our studies to a detailed analysis of a major component of the membrane core domain, DGI. Using inhibitors of glycoprotein processing and intracellular transport we show that DGI biosynthesis is a sequential process involving core glycosylation, oligosaccaride processing, entry into an insoluble pool, and final transport to the plasma membrane. These processes occur independently of cell-cell contact. However, in the presence of cell-cell contact, the rate and efficiency of transfer of DGI from the soluble into the insoluble pool, and the rate of transport to the plasma membrane is significantly higher. Cell-cell contact also results in the stabilization of the newly synthesized DGI at the plasma membrane ($t_{½}$ > 24 h). Taken together with our previous analysis of DPI/II, these results provide the first molecular insights into the regulation of cytoplasmic plaque and membrane core domain biosynthesis in desmosome assembly.

Materials and Methods

Cells

The morphology, growth characteristics, and culture conditions of the MDCK cells (clone No. 8) used in this study have been described previously (30). The degree of cell-cell contact in confluent monolayers of cells was modulated by adjusting the concentration of Ca^{++} in the growth medium (for details see reference 31).

Preparation of a Desmosome-enriched Fraction from Bovine Muzzle Epidermis

Desmosomes were purified from fresh bovine muzzle epidermis, and membrane core glycoproteins were separated from intracellular plaque proteins as described previously (45).

Preparation of an Antiserum against DGI

The glycoprotein fraction of bovine muzzle epidermis was separated on preparative SDS 5% polyacrylamide gels (23). The protein band corresponding to the 150,000-M_r (DGI) component of the desmosomes was well-separated from other proteins (see Fig. 1 *A*) and was excised from the gel, electroeluted from the gel slices (sample concentrator; ISCO, Inc., Lincoln, NE), and used to immunize a New Zealand white rabbit (30). After the second booster injection, serum was tested for antibody production by immunoblotting (see below). The IgG fraction of this antiserum was precipitated with $(NH_4)_2SO_4$ at 50% saturation and used in all further studies.

Immunoblotting

Proteins were transferred electrophoretically from SDS polyacrylamide gels to nitrocellulose filters as described previously (52). Filters were incubated with 1:1,000 dilution of antiserum followed by ^{125}I-protein A (10 μCi/μg) as described previously (30). Filters were exposed at −80°C to XAR-5 x-ray film using two intensifying screens (DuPont Co., Wilmington, DE).

Metabolic Labeling

Confluent monolayers of MDCK cells were established and maintained at 37°C in DME containing 5 μM Ca^{++} (LCM) or 1.8 mM Ca^{++} (HCM) on collagen-coated 35-mm petri dishes. For metabolic labeling (for details see reference 38), cells were preincubated in methionine-free medium for 30 min, and then were labeled metabolically with [^{35}S]methionine (1,200 Ci/mmol; New England Nuclear, Boston, MA) for 15 min in methionine-free LCM or HCM. The cells were then incubated in a >10,000 fold excess of unlabeled methionine (chase medium) in the appropriate growth medium. In some experiments inhibitors of glycoprotein processing (tunicamycin and monensin) were added to the appropriate growth medium before the metabolic labeling period. The inhibitor was included in the subsequent pulse-label and chase media. Stock solutions of tunicamycin (25 μg/ml) and monensin (25 mM) were made in DMSO.

To trypsinize the cell surface, cells were rinsed twice in a buffer containing 15 mM Tris-HCl, pH 7.5, 120 mM NaCl (Tris-saline), and then incubated at room temperature in 1 ml of trypsin solution (0.125% [wt/vol] in a buffer containing 137 mM NaCl, 5 mM KCl, 0.1% (wt/vol) glucose, 0.02% EDTA, pH 7.0, with $NaHCO_3$) for 2–5 min. The cell monolayer was monitored at all times by phase contrast microscopy. Trypsin digestion was stopped by the addition of 1 ml of FBS. The trypsin solution was removed by aspiration and the cell monolayer was washed twice with ice-cold Tris-saline containing 1 mM PMSF.

Cell Fractionation and DGI Immunoprecipitation

At each time point, cells were washed twice with ice-cold Tris-saline/PMSF and extracted at 4°C on the petri dish for 20 min in a buffer containing 10 mM Pipes (pH 6.8), 50 mM NaCl, 300 mM sucrose, 3 mM $MgCl_2$, 0.5% (vol/vol) Triton X-100, 1.2 mM PMSF, 0.1 mg/ml DNase, 0.1 mg/ml RNase (CSK buffer). $(NH_4)_2SO_4$ was added to a concentration of 250 mM and incubation was carried out for another 5 min (see reference 38 for details). The cells were scraped from the petri dish and the soluble and insoluble cell fractions were separated by centrifugation as described previously (38). Immunoprecipitation was performed as described in detail previously (38) with the following exception. Protein A–Sepharose CL-4B beads containing antigen–antibody complexes were washed successively as follows: first, the pellet was resuspended in 800 μl of HS buffer (15 mM Tris-HCl, pH 7.5, 5 mM EDTA, 2 mM EGTA, 1% [vol/vol] Triton X-100, 1% [wt/vol] Na-deoxycholate, 0.1% [wt/vol] SDS, 120 mM NaCl, 25 mM KCl, 0.1 mM DTT), underlayered with 200 μl of 1 M sucrose in HS buffer and centrifuged at 12,000 *g* for 1 min; second, the resulting pellet was resuspended in 1 ml of high salt immunoprecipitation wash buffer (HS buffer containing 1 M NaCl) and centrifuged as above; third, the resulting pellet was washed in low-salt buffer containing 10 mM Tris-HCl, pH 7.5, 2 mM EDTA, and 5 mM DTT. Analysis of the efficiency of immunoprecipitation indicated that >95% of DGI was precipitated under these conditions (data not shown).

For digestion with endo-β-*N*-acetylglucosaminidase H (endoH; Boehringer-Mannheim Biochemicals, Indianapolis, IN), the final pellet of protein A–Sepharose CL-4B beads containing the antigen–antibody complex was resuspended in 200 μl of endoH incubation buffer (20 mM sodium phosphate buffer, pH 6.0, 20 mM NaCl), and the sample was divided in half. To one half, 2.5 μU of endoH was added; the other half was the control and did not contain endoH. The samples were incubated at 4°C for 18 h.

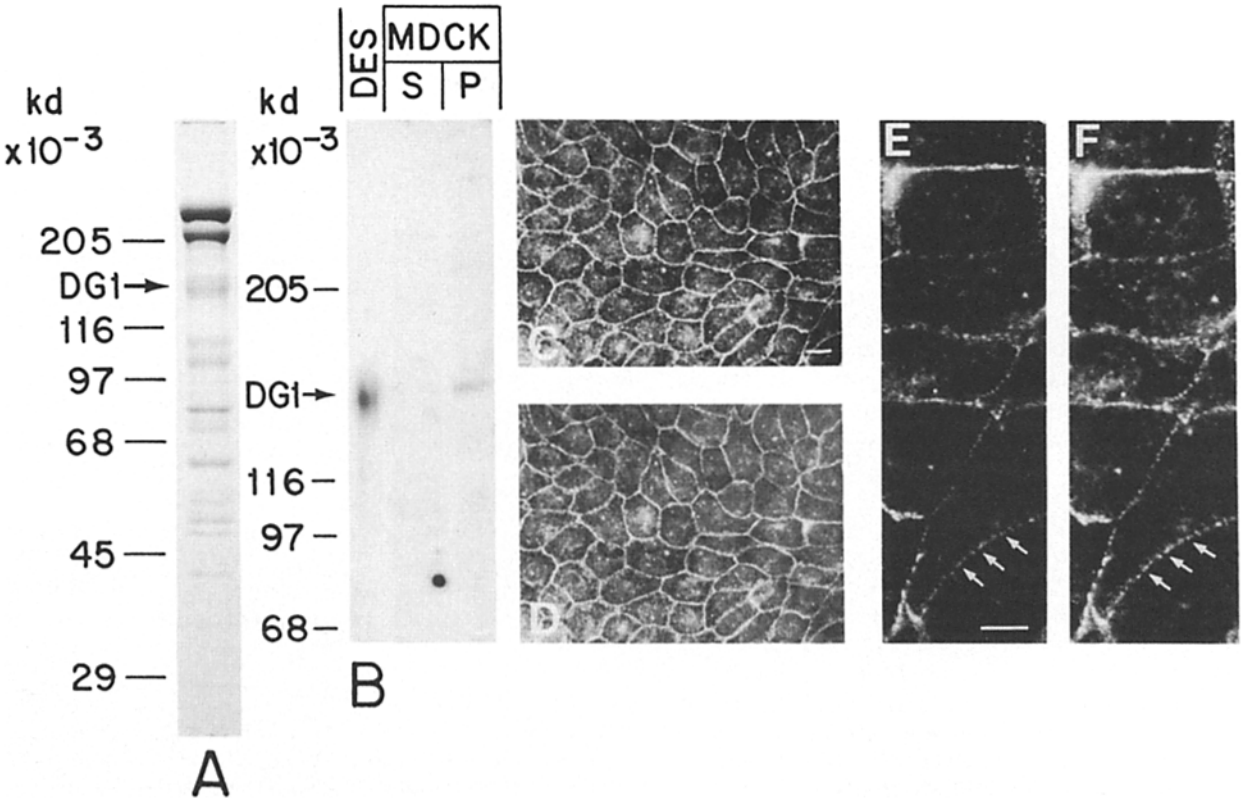

Figure 1. Characterization of an antiserum raised against DGI. (*A*) Coomassie blue-stained SDS/5–12.5% linear gradient polyacrylamide gel of purified desmosomes from bovine muzzle epidermis. Relative molecular mass markers: myosin (M_r = 205,000), β-galactosidase (M_r = 116,000), phosphorylase *b* (M_r = 97,000), BSA (M_r = 68,000), ovalbumin (M_r = 45,000), carbonic anhydrase (M_r = 29,000). The protein comprising the 150,000-M_r band (DGI) was purified and used as an antigen. (*B*) Autoradiogram of an immunoblot of total bovine epidermal desmosomal proteins (*Des*, lane 1) and of the soluble (*S*, lane 2) and insoluble (*P*, lane 3) fractions of MDCK cells with the DGI antiserum. The proteins in *B* were separated on an SDS 5% polyacrylamide gel. (*C–F*) Indirect double immunofluorescence of DGI and DPI/II in MDCK cell. Cells were cultured in HCM for 2 d, extracted with CSK buffer, and processed for double immunofluorescence as described in Materials and Methods. The same field of cells was photographed with matched filters for rhodamin, DGI (*C* and *E*), and fluorescein, DPI/II (*D* and *F*). Arrows indicate areas of codistribution of DGI and DPI/II. Bars: (*C* and *D*) 10 μm; (*E* and *F*) 5 μm.

At the end of the incubation, 900 μl of low-salt immunoprecipitation buffer were added, the samples were spun at 12,000 *g* for 2 min, and then washed twice with the same buffer. Immune complexes were boiled in SDS sample buffer and analyzed by SDS 5% PAGE and fluorography (38).

The relative amount of radioactivity in the band corresponding to DGI was determined from the resulting fluorograms by scanning densitometry using a Du-7 spectrophotometer (Beckman Instruments, Inc., Palo Alto, CA) equipped for automatic integrations; all x-ray films were preflashed (see references 30, 38) and several different exposures were analyzed. The data is expressed as normalized arbitrary units by summing the amounts of DGI quantitatively immunoprecipitated from the soluble and insoluble pools and then expressing the amount of DGI in each pool as a fraction of the total. In each case data from one typical experiment are presented, although all experiments were performed between three and five times.

Solubility Properties of DGI from MDCK Cells

Confluent monolayers of MDCK cells were established and maintained in replicate 35-mm petri dishes in LCM. Cells were pulse-labeled with [^{35}S]methionine for 15 min and then incubated in growth medium containing a >10,000-fold excess of cold methionine. After 1 or 2 h in chase medium, the cells were placed on ice, washed twice with ice-cold Tris-saline/PMSF, and then extracted for 5 min on a rocking platform at 4°C in buffer containing 10 mM Tris-HCl, pH 7.5, 2 mM EDTA, 0.1 mM DTT, 0.1 mM PMSF, and 25 mM KCl that included different concentrations of NaCl or Urea (see Fig. 5). Cells were scraped from the petri dishes in extraction buffer, centrifuged, and the soluble and insoluble fractions were processed for immunoprecipitation, SDS 5% PAGE, and fluorography as described above.

Indirect Immunofluorescence

Confluent monolayers of MDCK cells were established on collagen-coated coverslips. The cells were rinsed briefly in PBS and then either fixed and permeabilized in 100% methanol at −20°C, or extracted in CSK buffer and then fixed in 1.75% (vol/vol) formaldehyde and processed for indirect immunofluorescence as described in detail previously (39, 43). For double labeling, a mouse monoclonal antibody specific for epithelial DPI/II (Boehringer-Mannheim Biochemicals; 1:25 dilution in PBS) was applied together with the monospecific rabbit polyclonal prepared against DGI (1:100 dilution in PBS). The mouse antibody was visualized with biotinylated goat anti-mouse IgG and FITC-strepavidin. The rabbit antibody was visualized with rhodamine-conjugated anti-rabbit IgG. Alternatively cells were preincubated with wheat germ agglutinin (2 μg/ml; Sigma Chemical Co., St. Louis, MD) for 10 min at 4°C before fixation, and then the cells were processed for double immunofluorescence and successive additions of rhodamine conjugated wheat germ agglutinin (1/100 dilution in PBS; Sigma Chemical Co.) and DGI antibodies (visualized with biotinylated goat anti-rabbit IgG and FITC-streptavidin). Coverslips were mounted in Elvanol (42) and the cells viewed in a Zeiss Axiophot Microscope equipped with epifluorescence illumination.

Results

Characterization of the DGI Antibody

Immunoblotting of total proteins purified from bovine desmosome (Fig. 1 *B*) revealed that the antiserum raised against

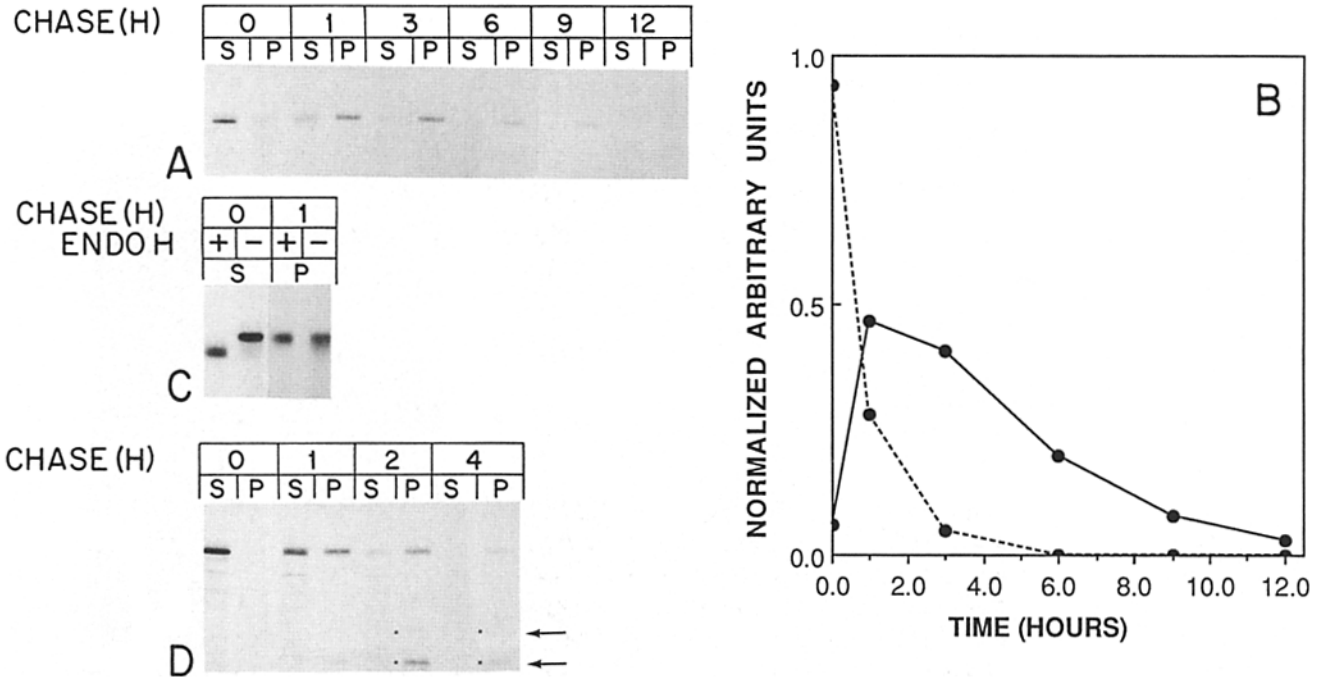

Figure 2. Synthesis, processing, and transport of DGI in confluent monolayers of MDCK cells grown in the absence of cell–cell contact. Confluent monolayers of MDCK cells were established and maintained in LCM for ~16 h. Cells were pulse-labeled with [^{35}S]methionine for 15 min and chased in LCM for up to 12 h (*A* and *B*). Duplicate petri dishes were treated with endoH (*C*) or 0.125% trypsin (*D*) as described in the text. Cells were extracted with CSK buffer and the soluble and insoluble fractions were immunoprecipitated with DGI antiserum and analyzed by SDS 5% PAGE, fluorography (*A*, *C*, and *D*), and scanning densitometry (*B*). (*A*) Tritration of the newly synthesized DGI from the soluble (*S*) into insoluble (*P*) pool during a chase period. (*B*) Quantitation of fluorogram shown in *A*. Newly synthesized DGI rapidly titrated from the soluble (- - -) into the insoluble pool (———) which in turn is degraded ($t_{½}$ < 4 h). (*C*) Glycosylation of newly synthesized DGI. At specific time points in the chase period, immunoprecipitated samples of DGI from soluble (*S*) or insoluble (*P*) protein pools were incubated with endoH (+) or without endoH (−) to determine the extent of complex glycosylation. (*D*) Appearance of the newly synthesized DGI at the cell surface. Transport of DGI to the plasma membrane was detected by trypsin digestion of DGI at the external cell surface. Digestion was detected by loss of DGI and the appearance of DGI tryptic fragments of 110,000 and 90,000 M_r (*arrows*).

Desmoglein I reacted with a single polypeptide band (M_r ~150,000) identified from previous studies as DGI (Fig. 1 *A*, lane *I*). To analyze MDCK cell proteins, confluent monolayers of MDCK cells were maintained in HCM for 2 d and then extracted with CSK buffer (see Materials and Methods). The resulting soluble and insoluble protein fractions were separated by centrifugation, and equivalent amounts of protein in each fraction were analyzed by SDS 5% PAGE and immunoblotting. The antiserum reacted with a single polypeptide band in the CSK buffer insoluble fraction; this protein had an electrophoretic mobility similar to that of DGI (Fig. 1 *B*, lane *3*). No immunoreactive protein was detected in the CSK buffer soluble pool (Fig. 1 *B*, lane *2*). Immunoprecipitation of extracts of whole MDCK cells revealed a single polypeptide of 150,000-M_r (see Figs. 2, 3, 5, 6, 7, 8, and 10), which also reacted with DGI antibodies in Western blots (data not shown). Indirect immunofluorescence staining of MDCK cells with DGI antiserum revealed a punctate pattern of staining at the plasma membrane of adjacent cells (Fig. 1, *C* and *E*). The preimmune serum gave little or no cell staining (data not shown). The staining pattern of DGI colocalized with that of Desmoplakin I/II observed in the same cells by double immunofluorescence staining (Fig. 1, *D* and *F*).

Fate of Newly Synthesized DGI in the Absence of Cell–Cell Contact

After 15-min pulse labeling with [^{35}S]methionine all of the newly synthesized DGI was present in a soluble pool of protein (Fig. 2 *A*, 0-min chase) and was sensitive to digestion with endoH (Fig. 2 *C*). Within 1 h of synthesis a portion (~50%) of the soluble pool of DGI entered a pool of protein which was insoluble in CSK buffer (Fig. 2, *A* and *B*). The portion of DGI remaining in the soluble pool was degraded very rapidly ($t_{½}$ ~ 30 min; Fig. 2 *B*). The insoluble pool of DGI was resistant to digestion with endoH (Fig. 2 *C*). The amount of newly synthesized DGI remaining in the insoluble pool during the chase period declined rapidly showing that in the absence of cell–cell contact DGI was metabolically unstable ($t_{½}$ < 4 h) (Fig. 2 *B*).

To determine whether DGI was transported to the plasma membrane in the absence of cell–cell contact, cells were treated with trypsin at various times during the chase period and the degradation of mature DGI and the concommitant appearance of DGI-specific tryptic fragments was determined by immunoprecipitation and fluorography. Two major tryptic fragments of DGI were detected (Fig. 2 *D*). A 110,000-M_r polypeptide appeared first upon addition of tryp-

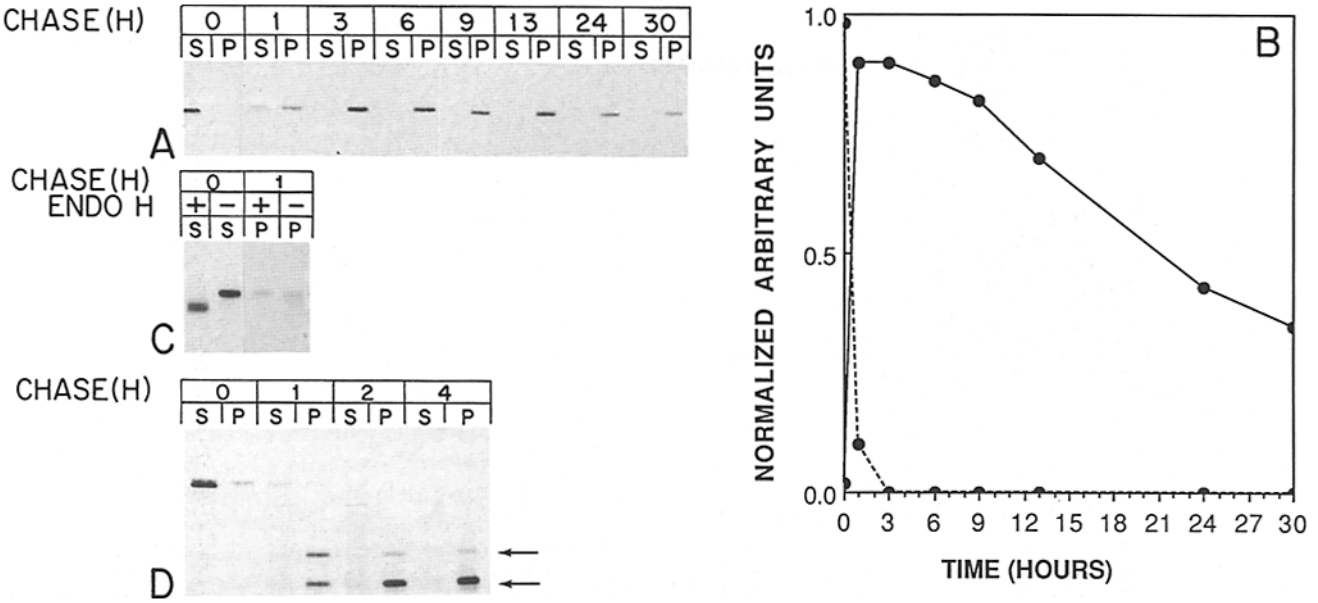

Figure 3. Synthesis, processing, and transport of the newly synthesized DGI in confluent monolayers of MDCK cells upon induction of cell-cell contact. Confluent monolayers of MDCK cells were established and maintained in LCM for 16 h when cell-cell contact was induced synchronously by replacing the LCM with HCM. 1 h later, cells were pulse-labeled with [^{35}S]methionine for 15 min and chased in HCM for up to 30 h as described in the legend to Fig. 2. (*A*) Tritration of newly synthesized DGI from the soluble (*S*) into insoluble (*P*) pool. (*B*) Fate of newly synthesized DGI during the chase period. The soluble pool of newly synthesized DGI (– – –) was rapidly and efficiently titrated into the insoluble pool (———). The insoluble pool of DGI was degraded with a $t_{½} \sim 24$ h. (*C*) Sensitivity of newly synthesized DGI in the soluble (*S*) or insoluble (*P*) pool to digestion with endoH (+). (*D*) The appearance of newly synthesized DGI at the plasma membrane was detected by trypsin digestion as described in the legend to Fig. 2. Newly synthesized, insoluble DGI appears at the plasma membrane within 1 h after chase as determined by the appearance of characteristic DGI tryptic fragments (*arrows*).

sin, and then was degraded to a 90,000-M_r protein which appeared to be resistant to further trypsin digestion (see also reference 40). Both tryptic fragments of DGI were detected in the insoluble protein fraction. DGI in the soluble pool was not sensitive to digestion by trypsin; therefore, we assume that this pool of DGI does not reach the plasma membrane (Fig. 2 *D*). This analysis revealed that trypsin-sensitive DGI was first detected 1 h after synthesis. Densitometric scanning of the fluorogram (Fig. 2 *D*) showed that at this time <10% of DGI was trypsin sensitive. Within 2 h, >50% of the DGI present in the cell was sensitive to digestion by trypsin.

These properties of DGI in confluent monolayers of cells grown in LCM appear to be the result of the lack of cell-cell contact rather than the effect of the low Ca^{++} concentration of the growth medium. Analysis of sparse, single cell cultures grown in HCM revealed similar kinetics of synthesis, processing, and degradation of DGI as those in confluent monolayers of cells grown in LCM (data not shown).

Fate of Newly Synthesized DGI upon Induction of Cell-Cell Contact

In the presence of cell-cell contact newly synthesized DGI initially entered a soluble pool of protein (Fig. 3, *A* and *B*) and was sensitive to endoH digestion (Fig. 3 *C*, 0-min chase). DGI was then rapidly ($t_{½} \sim 30$ min) and efficiently (>90%) titrated into the insoluble pool (Fig. 3, *A* and *B*) and became resistant to endoH digestion (Fig. 3 *C*, 1-h chase). Within 1 h, >90% of DGI was transported to the plasma membrane as determined by the appearance of trypsin-sensitive DGI on the cell surface (Fig. 3 *D*). Analysis of the amount of newly synthesized DGI remaining during a long chase period revealed that in the presence of cell contact DGI was metabolically stable ($t_{½} \sim 24$ h) (Fig. 3 *B*).

These results demonstrate that glycosylation, formation of an insoluble pool, and transport of DGI to the plasma membrane are independent of cell-cell contact. However, induction of cell-cell contact results in significant increases in the rates and efficiencies of these processes.

Recruitment of Newly Synthesized DGI into a Stable, Insoluble Pool upon Induction of Cell-Cell Contact

We analyzed the fate of the newly synthesized DGI in cells which initially did not have cell-cell contact but were subsequently induced to form cell-cell contact. As shown in Fig. 4, in the absence of cell-cell contact the soluble pool of newly synthesized DGI was titrated into an insoluble pool which in turn was degraded very rapidly ($t_{½} < 4$ h). However if cell-cell contact was induced 1 or 3 h after synthesis of this population of DGI, the portion of the newly synthesized pool of DGI that had not been degraded during the chase period in the absence of cell-cell contact now became metabolically stable ($t_{½} > 24$ h; Fig. 4). Thus, the metabolically unstable pool of DGI synthesized in the absence of cell-cell contact could be rapidly recruited into a stable pool upon induction of cell-cell contact.

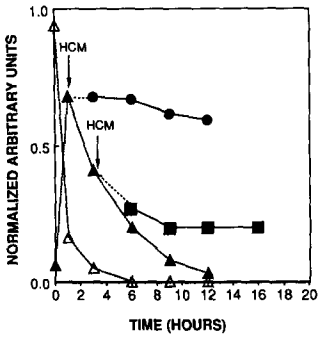

Figure 4. Recruitment of the newly synthesized DGI into a stable pool of protein upon induction of cell-cell contact. MDCK cells were established in LCM for 16 h, pulse-labeled with [^{35}S]methionine for 15 min, and chased either continuously in LCM (△, ▲) or induced to form cell-cell contact after 1 (●) or 3 h (■) by replacing the media with HCM. The amounts of [^{35}S]-methionine-labeled DGI in the CSK buffer soluble (△) and insoluble (▲, ●, ■) fractions were determined by immunoprecipitation, fluorography, and scanning densitometry.

Characterization of the Soluble and Insoluble Pools of Newly Synthesized DGI

A characteristic feature of DGI biosynthesis in the absence or presence of cell-cell contact is that DGI is found initially in a soluble pool of protein and is subsequently titrated into an insoluble pool. We have sought to characterize these two pools of newly synthesized DGI.

The soluble pool of DGI was analyzed by centrifugation on sucrose gradients (as described in reference 38). MDCK cells were established and maintained in LCM, pulse-labeled with [^{35}S]methionine and then incubated for a 15-min chase period. At this time ~75% of newly synthesized DGI was present in the soluble pool of protein that was extractable with CSK buffer (Fig. 2 *A*). Analysis of the sedimentation profile of soluble, newly synthesized DGI on sucrose gradients revealed a single, broad band of protein (data not shown). The peak fractions (11 and 12) had a sedimentation rate of ~7 S compared to standard proteins of known sedimentation values but the distribution of DGI was skewed to the bottom (heavy side) of the sucrose gradient (data not shown).

The insoluble pool of DGI was analyzed by testing for the extractability of DGI in buffers containing high salt or urea. MDCK cells were pulse-labeled with [^{35}S]methionine for 15 min and incubated for a chase period of 1 (Fig. 5 *D*) or 2 h (Fig. 5, *A–C*). At these times, ~50% and >85% of newly synthesized DGI, respectively, was present in the CSK buffer insoluble pool (Fig. 2). Replicate cultures of cells were extracted with buffers containing Triton X-100 and increasing concentrations of NaCl (Fig. 5 *A*) or urea (Fig. 5 *B*). After centrifugation, DGI was immunoprecipitated from the resulting soluble and insoluble pools of protein. DGI was relatively resistant to solubilization with buffers containing 0.5% (vol/vol) Triton X-100 and NaCl concentrations ranging from 0 mM (hypotonic) to 1 M; 1 M NaCl extracted <20% of DGI from the cells (Fig. 5, *A* and *C*). Extraction of cells in a buffer containing 0.5% Triton X-100 and 4 M urea also resulted in the solubilization of <25% of DGI (Fig. 5, *B* and *C*). However, extraction with a buffer containing 6 M urea resulted in the solubilization of ~60% of the DGI (Fig. 5, *B* and *C*). Similar results were obtained when cells were ex-

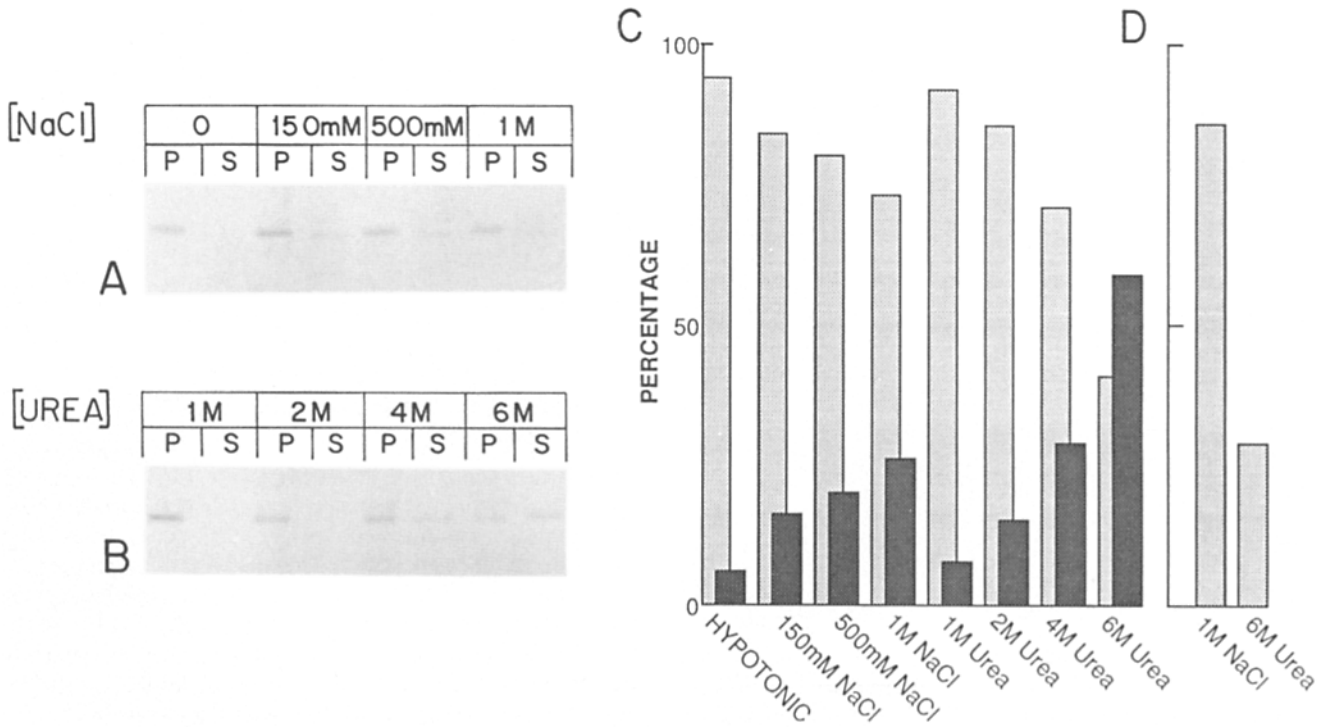

Figure 5. Extractability of DGI from MDCK cells. Confluent monolayers of MDCK cells were established and maintained in LCM for 16 h, metabolically labeled with [^{35}S]methionine for 15 min, and chased in LCM for either 1 (*D*) or 2 (*A–C*) h. Cells were extracted on the petri dish in a buffer containing 0.5% Triton X-100 and increasing concentrations of NaCl (*A*) or urea (*B*) (for details, see Materials and Methods). The resulting soluble (*S*) and insoluble (*P*) fractions were immunoprecipitated with DGI antiserum and analyzed by SDS 5% PAGE and fluorography (*A* and *B*). The fluorograms were quantitated by scanning densitometry, and the percentage of total DGI in the soluble (heavy stipling) and insoluble fractions (light stipling) was expressed in the form of a histogram (*C* and *D*).

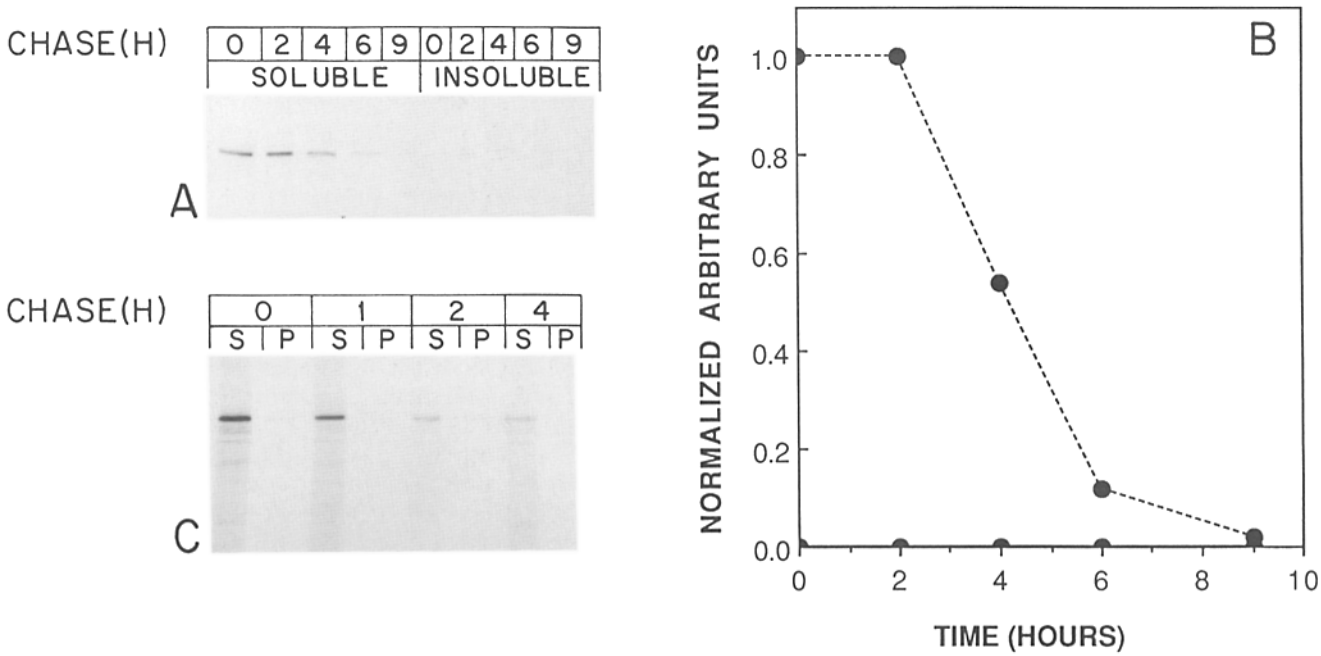

Figure 6. Synthesis, processing, and transport of DGI in confluent monolayers of MDCK cells grown in the presence of tunicamycin and absence of cell–cell contact. Confluent monolayers of MDCK cells were preincubated in LCM containing 2.5 μg/ml tunicamycin for 2 h. Cells were pulse-labeled with [^{35}S]methionine for 15 min and chased in presence of 2.5 μg/ml tunicamycin. (*A*) Partitioning of DGI in the soluble and insoluble pools during the chase period. (*B*) Quantitation of the fluorogram in *A*; soluble pool (– – –), insoluble pool (———). (*C*) Resistance of DGI to digestion by extracellular trypsin; note that the characteristic tryptic fragments of DGI digestion are not detected (for comparison see Fig. 2 or 3); the decrease in the amounts of DGI are due to cellular degradation of this protein.

tracted either 1 (Fig. 5 *D*) or 2 h (Fig. 5 *C*) after pulse-labeling with [^{35}S]methionine.

The Biosynthetic Pathway of DGI in MDCK Cells: Dissection of Stages Using Inhibitors of Glycoprotein Processing and Transport

Our analysis of DGI synthesis in MDCK cells grown in the absence or presence of cell–cell contact have shown that DGI is complex glycosylated and enters an insoluble pool of protein before arrival at the plasma membrane. We have sought to determine the sequence and intracellular location of stages of DGI biosynthesis and transport to the plasma membrane using general inhibitors of glycoprotein processing and transport.

Effects of Inhibiting DGI Core Glycosylation with Tunicamycin

Replicate 35-mm petri dishes of confluent monolayers of MDCK cells were established and maintained in LCM for ~16 h. The growth media was replaced with LCM containing 2.5 μg/ml tunicamycin (Figs. 6 and 7), an inhibitor of N-linked core glycosylation (18, 51). 1 h later the growth media in one set of petri dishes were replaced with HCM containing 2.5 μg/ml tunicamycin (Fig. 7). The incubation was continued for another hour in both sets of cultures. Cells were pulse-labeled with [^{35}S]methionine and chased in appropriate growth medium containing tunicamycin for up to 13 h. At specific time points during the chase period, cells were extracted with CSK buffer. An additional set of petri dishes containing LCM or HCM and tunicamycin were treated with trypsin to determine the presence of DGI at the cell surface (Figs. 6 *C* and 7 *C*). DGI was immunoprecipitated from the soluble and insoluble fractions and analyzed by SDS 5% PAGE, fluorography, and scanning densitometry (Figs. 6, *A*, *B*, and *C* and 7, *A*, *B*, and *C*).

In the absence (Fig. 6) or presence (Fig. 7) of cell–cell contact, tunicamycin inhibited core glycosylation of newly synthesized soluble DGI by the following criteria: (*a*) there was no decrease in the electrophoretic mobility of DGI commensurate with core glycosylation; (*b*) there was no effect of incubation with endoH on the electrophoretic mobility of DGI (data not shown); and (*c*) there was no incorporation of [^{3}H]glucosamine into DGI (data not shown).

In the absence of cell–cell contact, DGI appeared in the soluble pool of protein upon synthesis but was not titrated into the insoluble pool at any time during the chase period (Fig. 6 *A*). In addition, newly synthesized DGI was not transported to the plasma membrane as determined by the fact that it was resistant to extracellular trypsin digestion (Fig. 6 *C*). Analysis of the amounts of newly synthesized DGI remaining during the chase period showed that the protein was degraded very rapidly ($t_{1/2}$ < 3 h; Fig. 6 *B*).

In the presence of cell–cell contact, as in the absence of cell–cell contact, tunicamycin inhibited core glycosylation of the newly synthesized DGI (Fig. 7 *A*). However, in contrast to the effects in cells without cell–cell contact treatment with the drug in the presence of cell contact showed no effect on either the rate ($t_{1/2}$ ~ 30 min) or efficiency (>90%) of titration of newly synthesized DGI from the soluble into the insoluble pool (Fig. 7 *B*) as compared to control cultures (for comparison see Fig. 3). Furthermore, the unglycosylated in-

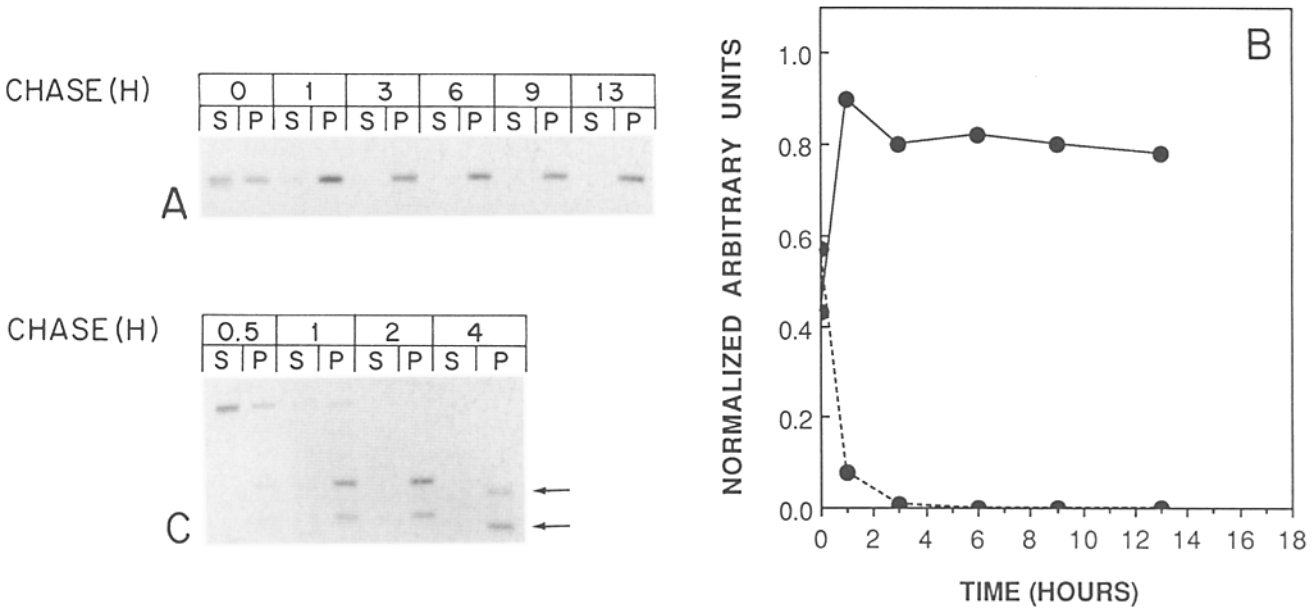

Figure 7. Synthesis, processing, and transport of the newly synthesized DGI in confluent monolayers of MDCK cells grown in presence of tunicamycin and cell-cell contact. Confluent monolayers of MDCK cells were established in LCM and then preincubated with 2.5 μg/ml tunicamycin in LCM for 1 h. The medium was replaced with HCM (containing 2.5 μg/ml tunicamycin) to synchronously induce cell-cell contact. After 1 h, the cells were pulse-labeled with [^{35}S]methionine and chased in the presence of tunicamycin. (*A*) Titration of newly synthesized DGI from the soluble (*S*) into the insoluble (*P*) pool during the chase period. (*B*) Quantitation of the fluorogram in *A*; soluble pool (- - -), insoluble pool (———). (*C*) Sensitivity of DGI to trypsin digestion during the chase period; note the appearance of DGI tryptic fragments (*arrows*).

soluble pool of DGI was rapidly transported to the plasma membrane (within 1 h of synthesis), as determined by the sensitivity of DGI to extracellular trypsin digestion (Fig. 7 *C*). At the plasma membrane, DGI was metabolically stable ($t_{½}$ > 24 h; Fig. 7 *B*).

Effects of Inhibiting DGI Transport between the Golgi Complex and Plasma Membrane with Monensin

Confluent monolayers of MDCK cells were established and maintained in LCM for ~16 h and then the growth medium was changed to HCM for 1 h. Cells were preincubated for 30 min in the presence of 25 μM monensin or 25 μM monensin and 2.5 μg/ml tunicamycin. Monensin is an ionophore which inhibits the transport of membrane glycoproteins between the Golgi complex and plasma membrane (19, 49, 50). Replicate 35-mm petri dishes were pulse-labeled with [^{35}S]methionine and chased for up to 4 h in HCM containing monensin or monensin and tunicamycin. Control cells were pulse-labeled and chased in the absence of the inhibitor.

In the presence of cell-cell contact and monensin newly synthesized DGI was core glycosylated (endoH-sensitive), became complex glycosylated (endoH-resistant), and entered the insoluble pool with kinetics similar to the control (data not shown). However, the majority of the insoluble pool of DGI synthesized in the presence of monensin was not transported to the plasma membrane (Fig. 8). In the absence of inhibitors (Fig. 8), 100% of the insoluble pool of DGI became sensitive to extracellular trypsin demonstrating transport of the protein to the plasma membrane. In MDCK cells treated with monensin, only ~25% of newly synthesized DGI became sensitive to extracellular trypsin indicating that

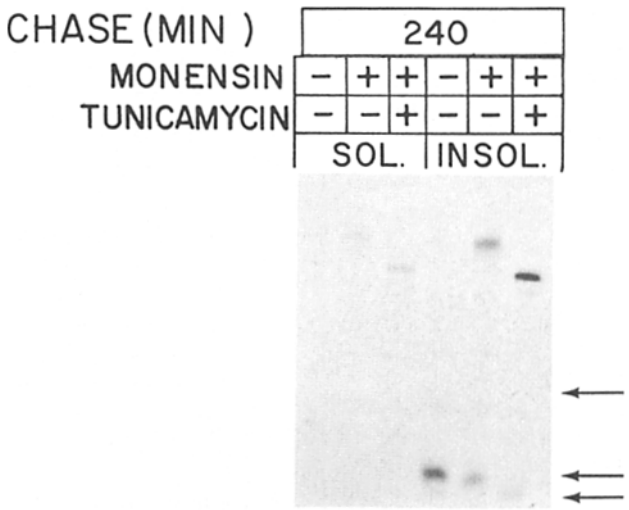

Figure 8. Intercompartmental transport of DGI in MDCK cells grown in presence of cell-cell contact and inhibitors of core glycosylation (tunicamycin) and glycoprotein transport (monensin). Confluent monolayers of MDCK cells were pulse-labeled with [^{35}S]methionine and chased in either HCM (control), HCM containing 25 μM monensin, or HCM containing 2.5 μg/ml tunicamycin and 25 μM monensin. Triplicate petri dishes were treated with extracellular trypsin at the conclusion of a 240-min chase period. Arrows indicate the appearance of the tryptic fragments; scanning densitometry shows that >75% of DGI is resistant to trypsin digestion in cells treated with monensin, and >90% is resistant in cells treated with monensin and tunicamycin. Note also the differences in electrophoretic mobility of DGI tryptic fragments in the cells treated with tunicamycin compared to the control due to the inhibition of core glycosylation.

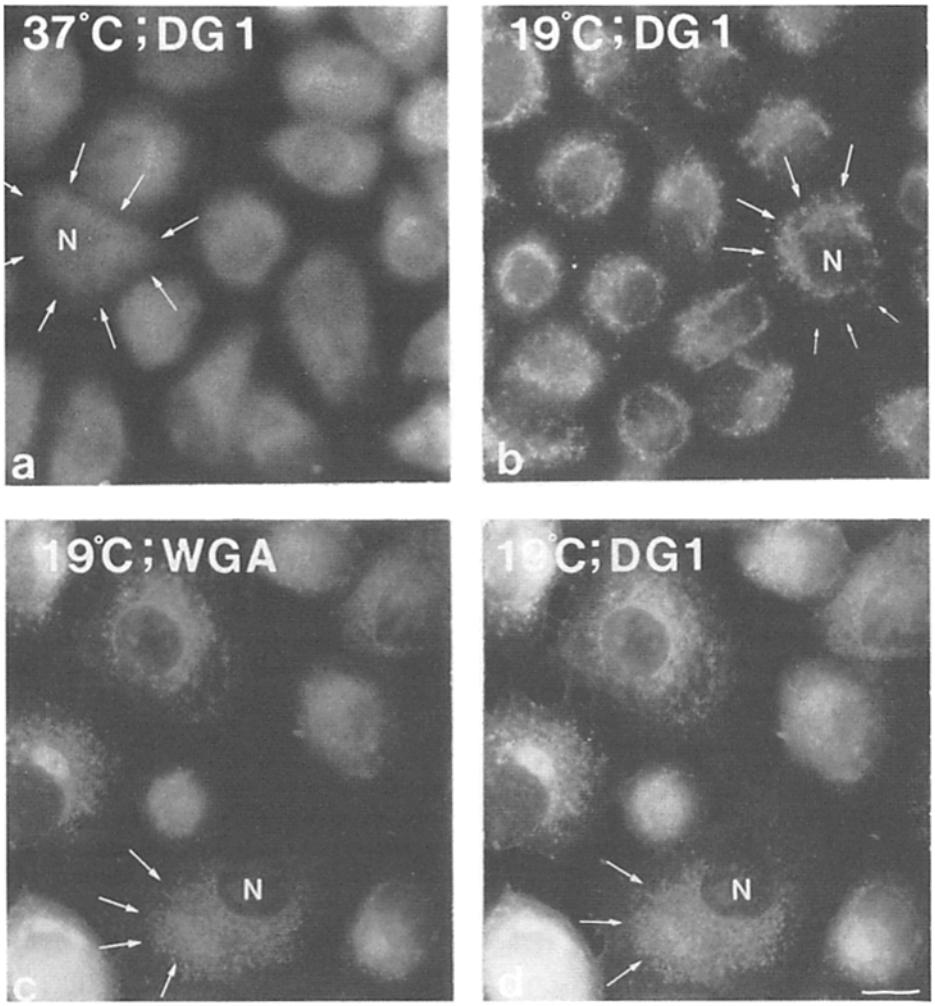

Figure 9. Indirect immunofluorescence of DGI in MDCK cells maintained at 37°C or 19°C. Cultures of MDCK cells were established and maintained at 37°C (*a*) or transferred to 19°C overnight (*b*, *c*, and *d*). For single immunofluorescence staining of DGI (*a* and *b*), cells were fixed and permeabilized in 100% methanol at −20°C and then processed as described in Materials and Methods. For double fluorescence labeling of the Golgi complex (*c*) and DGI (*d*) in the same cells, cultures of MDCK cells at 19°C were preincubated with wheat germ agglutinin for 10 min at 4°C to saturate the plasma membrane binding sites. Cells were fixed and permeabilized as described above, and then incubated first with rhodamine-labeled wheat germ agglutinin and then with DGI antibodies followed by biotinylated goat anti-rabbit IgG and FITC-avidin. The same field of cells were photographed with matched filters for rhodamine (*c*) and fluorescein (*d*). Bar, 20 μm.

~75% of the protein remained intracellular. The fraction of DGI transported to the plasma membrane may be due to leakiness in the inhibition of vesicle transport by monensin. It is noteworthy that in MDCK cells treated with monensin and tunicamycin >90% of newly synthesized unglycosylated DGI was not transported to the plasma membrane (Fig. 8).

Effects of Blocking DGI Processing and Transport in the Golgi Complex at 19°C

To investigate intermediate stages in the transport of DGI to the membrane we have used a reduced temperature assay which slows down or prevents the transport of membrane glycoproteins between the stacks of the Golgi complex and the cell surface (25).

Indirect immunofluorescence of MDCK cells maintained in LCM at either 37°C or 19°C shows dramatic differences in the distribution of DGI. At 37°C DGI exhibits a uniform, diffuse staining over the whole cell which extends to cell periphery (Fig. 9 *a*, *arrows*). There is little or no staining of subcellular compartments. However, MDCK cells incubated at 19°C exhibit an intense perinuclear staining (Fig. 9 *b*, *arrows*). The staining is localized to the cytoplasm on one side of the nucleus. Note that there is little or no diffuse staining of the cell periphery in comparison to that in the control (Fig. 9 *a*). We suggest that this difference in staining is due to the fact that DGI present at the plasma membrane at the start of the 19°C block had been degraded ($t_{1/2} \sim 3$ h) during the overnight incubation at 19°C. At the same time, newly synthesized DGI accumulated in an intracellular compartment and was not transported to the plasma membrane (see below). Double staining of MDCK cells with DGI antibodies and rhodamin-labeled wheat germ agglutinin (Fig. 9 *c*), which labels the Golgi complex (43), revealed very similar perinuclear staining patterns (Fig. 9, *c* and *d*, *arrows*). These results indicate that at 19°C DGI accumulates in the Golgi complex (see below).

To determine the effect of 19°C on the transport and processing of newly synthesized DGI, cells were pulse-labeled with [^{35}S]methionine for 10 min at 37°C in LCM or HCM. The medium was removed and the cells rinsed twice in chase medium precooled to 19°C. The cells were immediately transferred to an incubator at 19°C and chased in the appropriate media for up to 180 min. At this time, duplicate plates were rinsed in growth medium warmed to 37°C and then returned to an incubator at 37°C. The chase period was continued for a further 10 or 30 min. DGI processing was determined by analysis of soluble and insoluble cell fractions by immunoprecipitation (Fig. 10, *A* and *B*) and resistance to en-

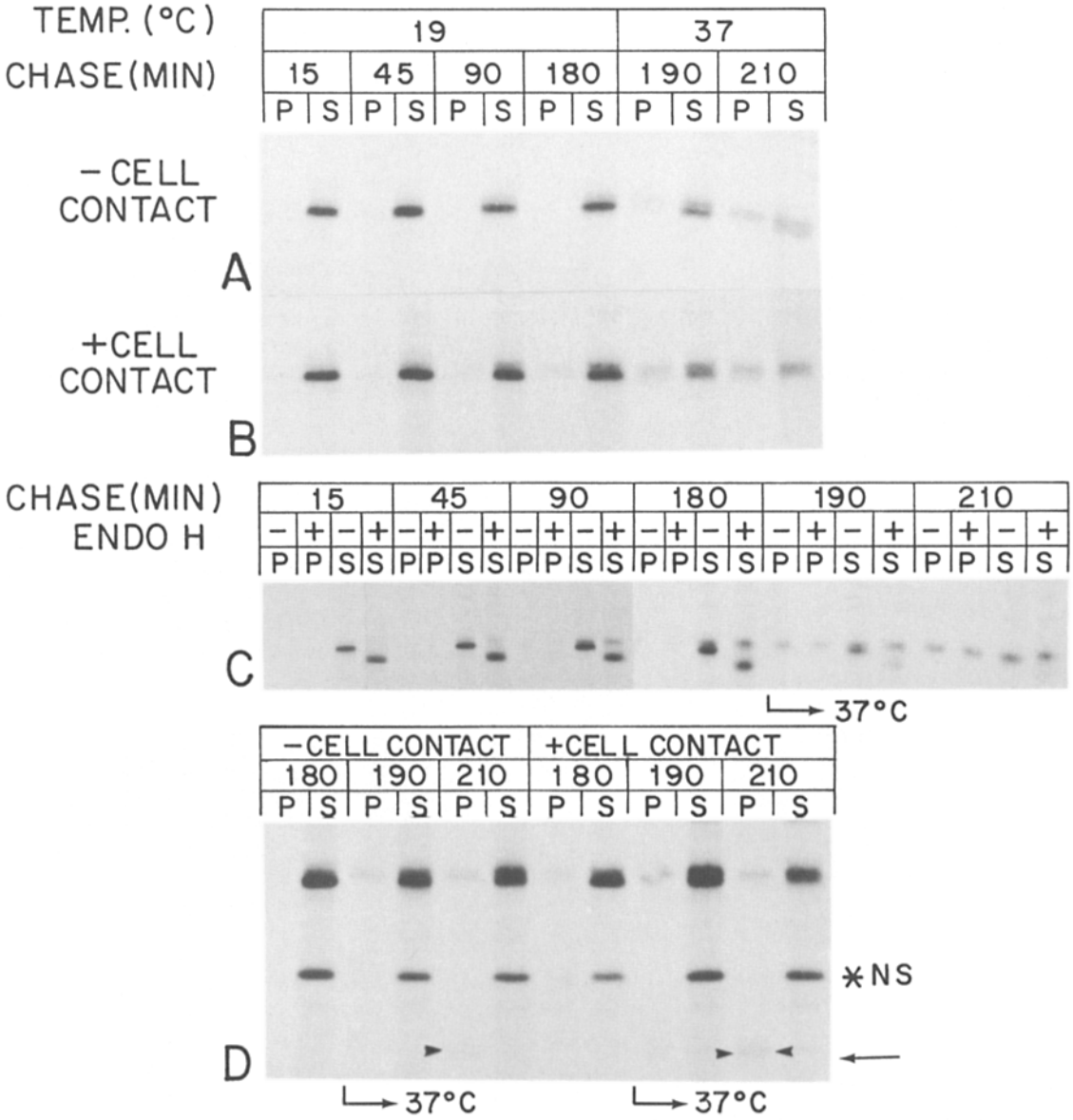

Figure 10. Synthesis, processing, and transport of DGI in MDCK cells grown at 19°C. Confluent monolayers of MDCK cells were established and maintained in LCM for 16 h. Cells were pulse-labeled with [^{35}S]methionine in either LCM (*A*) or HCM (*B*) at 37°C for 10 min and immediately transferred to 19°C where they were incubated for a chase period of up to 180 min. After 180 min duplicate plates were returned to 37°C and the chase was continued for another 10 or 30 min. Cells were digested on the petri dish with trypsin as described in Materials and Methods. Cells were extracted with CSK buffer and the resulting soluble and insoluble fractions were immunoprecipitated with DGI antiserum. Immunoprecipitated samples from the set of cultures incubated in HCM were divided in half, and one-half was digested with endoH and the other half was used as control (*C*); duplicated plates were also treated with trypsin (*D*). Immunoprecipitated samples were analyzed by SDS 5% PAGE and fluorography. (*A* and *B*) Fluorograms of DGI immunoprecipitates from MDCK cells grown in the absence (*A*) or presence (*B*) of cell–cell contact for 180 min at 19°C and subsequently for 10 or 30 min at 37°C (insoluble pool [*P*], soluble pool [*S*]) (*C*) Soluble (*S*) and insoluble (*P*) fractions of MDCK cells grown in the presence of cell contact for 180 min at 19°C and then 10 or 30 min at 37°C were immunoprecipitated and digested with endoH (+). (*D*) Cells grown in the absence or presence of cell contact were treated with trypsin at different times of the chase period (180 min at 19°C, or subsequent times of 10 or 30 min at 37°C). Arrows indicate the 110,000-M_r tryptic fragment of DGI. *NS*, nonspecific protein coimmunoprecipitated with DGI antiserum.

doH digestion (Fig. 10 *C*). Transport and appearance of newly synthesized DGI at the plasma membrane was determined by the sensitivity of proteins to trypsin digestion at the cell surface (Fig. 10 *D*).

Incubation of MDCK cells at 19°C resulted in the core glycosylation of newly synthesized DGI (Fig. 10, *A–C*; 15–180 min) but blocked complex glycosylation as determined by the sensitivity of DGI to digestion by endoH throughout the incubation time (Fig. 10 *C*). In addition, the 19°C incubation inhibited the titration of DGI from the soluble to the insoluble pool (Fig. 10, *A* and *B*; 15–180 min chase) and the transport of DGI to the cell surface (Fig. 10 *D*; 180 min ± cell–cell contact). Note that in the controls, all of the newly synthesized DGI was processed and transported to the cell

surface within 180 min (see Figs. 2 *D* and 3 *D*). The inhibition of DGI processing and transport in the Golgi complex at 19°C occurred in the presence or absence of cell–cell contact (Fig. 10).

Upon raising the temperature to 37°C, the inhibition of DGI processing and transport was lifted. However, further processing of DGI occurred in a precise sequence. 10 min after raising the temperature to 37°C, there was a significant increase in amount of a new DGI protein band in the soluble pool with an electrophoretic mobility slower than that of the core glycosylated, endoH-sensitive form of DGI (Fig. 10, *A* and *B*). This new protein band was resistant to digestion by endoH (Fig. 10 *C*) indicating that trimming of high mannose and addition of complex sugars had been initiated in the soluble pool of protein. Next, we detected endoH-resistant DGI in the insoluble pool (Fig. 10 *C*). This temporal sequence is most clearly observed in the samples from cells without cell–cell contact (Fig. 10 *A*); in the presence of cell contact, the kinetics of complex glycosylation and entry into the insoluble pool are faster and more difficult to uncouple. Analysis of the sensitivity of DGI to trypsin digestion at the cell surface revealed that little or no DGI was present at the plasma membrane 10 min after raising the temperature to 37°C. However, after 30 min, a small portion of newly synthesized DGI in the insoluble pool had become sensitive indicating that transport of DGI to the plasma membrane had been initiated. After 1 h at 37°C, all of the DGI was trypsin sensitive (data not shown).

Discussion

Previous studies have characterized the substructure of the desmosome in great detail and have shown that it is composed of two domains, a cytoplasmic plaque and a membrane core, each of which has a distinct morphology and protein composition (for references, see the introduction to the article). These studies provide the foundation for our analysis of the biosynthesis of proteins of these domains and the regulation of their assembly into desmosomes. We recently reported the results of our detailed analysis of two major components of the cytoplasmic plaque domain, DPI/II (38, 39). We have now extended this analysis to a major component of the membrane core domain, DGI. The experimental design is similar in both studies, which allows us to compare the kinetics of biosynthesis and processing of these different proteins. Our experimental approach to the analysis of DGI biosynthesis has involved the dissection of the stages of processing and transport of the newly synthesized protein to the plasma membrane. An understanding of the sequence of these stages will allow us to ask questions about the mechanisms that regulate DGI transport and assembly, as well as those that regulate the coordinate assembly of the membrane core and cytoplasmic plaque domains during the formation of desmosomes.

Sequential Stages in DGI Processing and Transport to the Plasma Membrane

Upon synthesis, DGI is present exclusively in a pool of protein which is soluble in a buffer containing Triton X-100 and a high concentration of salt, CSK buffer (Figs. 2 and 3). Analysis of the soluble pool of DGI on sucrose gradients shows that the protein has a sedimentation value of 7.0–7.5 S (data not shown). The soluble pool of DGI is sensitive to digestion with endoH (Figs. 2 and 3) an enzyme that cleaves the high mannose precursor oligosaccharide of core glycosylated proteins (48). Tunicamycin blocks glycosylation of DGI (Figs. 6 and 7; see also reference 40); this drug inhibits the synthesis of the dolichol-pyrophosphate–linked oligosaccharide precursor that is required for core glycosylation of proteins in the endoplasmic reticulum (9). From these results, we conclude that the soluble pool of core-glycosylated DGI is formed in the endoplasmic reticulum.

Transport of the soluble pool of newly synthesized DGI from the endoplasmic reticulum to the Golgi complex was detected by the appearance of DGI that was resistant to digestion with endoH (Figs. 2 and 3). Previous studies have shown that glycoproteins are resistant to endoH digestion after trimming of the high mannose precursor oligosaccharide and addition of the first terminal GlcNAc residue (48). Significantly, the enzyme involved in the addition of the GlcNAc residue, GlcNAc-transferase I, has been localized to the medial stacks of the Golgi complex (11). Hence, resistance to endoH digestion marks kinetically the point in time that DGI passes through the medial stacks of the Golgi complex. This is significant because we have found that DGI enters an insoluble pool of protein at about the time resistance to digestion by endoH is acquired (Figs. 2 and 3).

The insoluble pool of newly synthesized DGI is not extracted from MDCK cells in buffers containing Triton X-100 and either 1 M NaCl or 4 M urea (Fig. 5). These properties are similar to those of DGI in whole desmosomes isolated from bovine keratinocytes (45), and of DGI at steady-state in MDCK cells, which has been localized to desmosomes as shown by immunofluorescence microscopy (Fig. 1). Significantly, however, the insoluble pool of newly synthesized DGI in MDCK cells is formed in the presence or absence of cell–cell contact (Figs. 2 and 3), and before the protein is transported to the plasma membrane (see below). We conclude that the formation of the insoluble pool is not a consequence of arrival of DGI at the plasma membrane or its assembly into desmosomes.

Where in the cell does DGI become insoluble? Our detailed kinetic analysis allows us to define in some detail the intracellular component involved. We found that incubation of MDCK cells at 19°C blocked the normal transfer of newly synthesized DGI into the insoluble pool and inhibited the acquisition of endoH resistance (Fig. 10). Based on this result we suggest that, under these conditions of incubation, DGI had not reached the site of GlcNAc-transferase I in the medial stack of the Golgi complex (see above). It is a formal possibility that GlcNAc-transferase I activity could be reduced or inhibited at 19°C. However, similar studies have shown that hemagglutinin is complex glycosylated under these conditions (25) indicating that GlcNAc-transferase I is active at 19°C in MDCK cells; we do not know the reason for the different effects of 19°C on the processing of these two glycoproteins. Although, these experiments do not enable us to pinpoint the subcellular location of the 19°C block in newly synthesized DGI transport, indirect immunofluorescence of the steady-state pool of DGI at 19°C shows intense staining of DGI at the Golgi complex (Fig. 9). Upon raising the temperature to 37°C, we showed that endoH-resistant form of DGI first appeared in the soluble pool and then began to enter

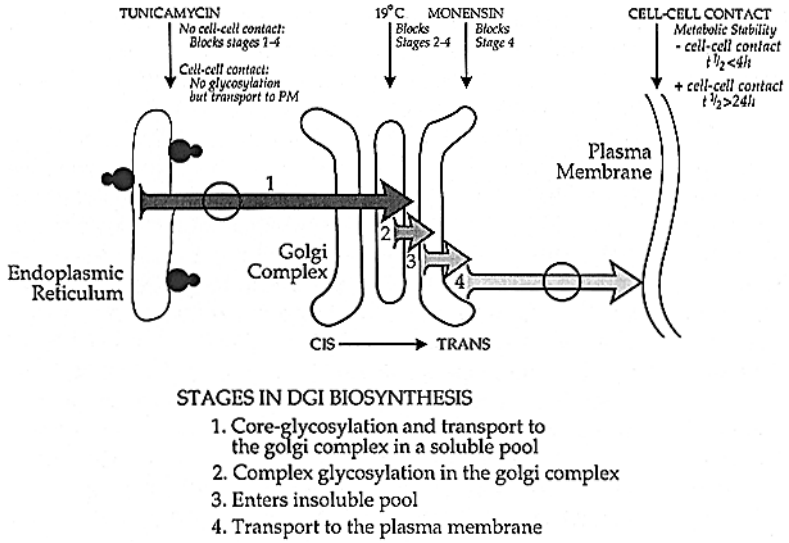

Figure 11. Schematic diagram of the stages involved in the biosynthetic pathway of DGI in MDCK epithelial cells and the stages blocked by various inhibitors of glycoprotein processing and transport. For details, see the text.

the insoluble pool (Fig. 10). This indicates that kinetically the insoluble pool of DGI is formed after complex glycosylation of DGI is initiated and, therefore, is located distal to the medial stack of the Golgi complex.

To determine more precisely the location of the insoluble pool we used the results of the experiment with the ionophore monensin (Fig. 8), which inhibits transport of vesicles from the Golgi complex to the plasma membrane (49, 50). The results showed unequivocally that in the presence of monensin newly synthesized DGI was endoH resistant and insoluble, but was not transported to the plasma membrane (Fig. 8). Taken together with the results of the 19°C experiment, our data indicate that transfer of newly synthesized DGI from the soluble to insoluble pool of protein occurs in a compartment located between the medial stack of the Golgi complex and the vesicles which transport proteins from the Golgi complex to the plasma membrane.

Effects of Cell–Cell Contact on DGI Biosynthesis

Previously, morphological studies have shown that cell–cell contact results in the rapid assembly of desmosomes at the plasma membrane of adjacent cells. Our studies on the biosynthesis of DGI show that cell–cell contact has significant effects on the rates and efficiencies of titration of the soluble into insoluble pool and transport of newly synthesized insoluble DGI to the plasma membrane, and it is also a critical determinant of the metabolic stability of newly synthesized DGI.

In the absence of cell–cell contact and desmosome assembly only ~50% of newly synthesized DGI is transferred to the insoluble pool 60 min after synthesis (Fig. 2). The remaining portion of DGI is degraded very rapidly in the soluble pool ($t_{½}$ ~ 30 min). This indicates that, in the absence of desmosome assembly, the insoluble pool of DGI has a limited capacity. However, upon induction of cell–cell contact and desmosome assembly, we found that the rate of transfer of newly synthesized DGI to the insoluble pool increased approximately twofold, and that >90% of the soluble pool was titrated into the insoluble pool by 1 h (Fig. 3). Thus, the capacity of the insoluble pool of DGI increases substantially upon cell–cell contact. Cell–cell contact also increases the rate (1 h vs. 2 h) and efficiency (>90% vs. ~50%) of transport of the newly synthesized insoluble DGI to the plasma membrane (see below).

In addition, we found that the metabolic stability of newly synthesized DGI is strictly dependent upon cell–cell contact (Figs. 2 and 3; see also reference 41). In the absence of cell–cell contact newly synthesized DGI is transported to the plasma membrane and is degraded rapidly ($t_{½}$ < 4 h). In the presence of cell–cell contact this pool of DGI becomes metabolically stable ($t_{½}$ > 24 h). Since DGI is colocalized with DPI/II in desmosomes after cell–cell contact (Fig. 1), we assume that the metabolic stability of DGI correlates with the assembly of the protein into desmosomes. At present, we do not know the nature of the degradative process that removes DGI from the plasma membrane in the absence of desmosome formation. However, our experiments show that newly synthesized DGI remains at the plasma membrane in the absence of desmosome assembly, since induction of cell–cell contact at intervals of 1 or 3 h after synthesis results in the stabilization of DGI (Fig. 4). This result indicates that in the absence of desmosome formation, newly synthesized DGI does not appear transiently at the plasma membrane and is then internalized and degraded, but remains at the plasma membrane in a state that can be assembled and stabilized into desmosomes upon cell–cell contact up to 3 h after synthesis.

Regulation of DGI Processing and Transport to the Plasma Membrane

The results of this study indicate that the biosynthetic pathway of DGI comprises four stages (see Fig. 11): (*a*) formation of a soluble pool of core-glycosylated DGI in the endoplasmic reticulum; (*b*) transport of this pool of protein to the Golgi complex and the completion of complex glycosylation; (*c*) titration of complex glycosylated protein into an insoluble pool; and (*d*) transport of the insoluble pool from the Golgi complex to the plasma membrane. The definition of these stages is useful since it provides a basis for deducing the regulation of DGI transport and assembly.

When MDCK cells were grown in the presence of cell–cell

contact and the inhibitor tunicamycin we showed that newly synthesized DGI is not core or complex glycosylated (Figs. 6 and 7; see also reference 40). However, DGI is transferred from the soluble to the insoluble pool of protein and is transported to the plasma membrane with similar kinetics as in control cells. It was a formal possibility that DGI was transported to the plasma membrane by an unconventional route, for instance, directly from the endoplasmic reticulum to the plasma membrane. However, we showed that in the presence of tunicamycin and monensin newly synthesized DGI was inhibited from transport to the plasma membrane (Fig. 8). This result strongly indicates that in the presence of tunicamycin DGI was transported to the plasma membrane via the Golgi complex.

This result has several implications for understanding the role of glycosylation and intracellular transport in DGI biosynthesis. First, this result indicates that glycosylation per se is not an obligatory step required for the transfer of newly synthesized DGI to the insoluble pool or its transport to the plasma membrane. Thus, it is unlikely that transfer of DGI to the insoluble pool is a consequence of conformational changes in the protein that might occur through N-linked glycosylation. Rather, the results imply that the formation of the insoluble pool of DGI is a consequence of the protein reaching a specific intracellular location in the biosynthetic pathway (e.g., transit through the late Golgi complex). It is possible that DGI undergoes another form of posttranslational modification at this location that renders it insoluble. Alternatively, DGI may form a complex with other proteins of the desmosome at this location that results in the increased insolubility of the protein; as noted earlier, the insoluble pool of newly synthesized DGI has properties similar to that of the membrane core domains in fully assembled desmosomes. The second implication of these results is that DGI glycosylation is not required for targeting the protein to the plasma membrane and the formation of desmosomes. This is in agreement with earlier studies by Overton (37), who showed that desmosomes were formed in cultures of explanted epithelial cells grown in the presence of tunicamycin.

The present results do not allow us to make any definitive conclusion about whether entry into the insoluble pool is required for transport to the plasma membrane. However, there is correlative evidence to indicate that this may be the case. First, we never detected the soluble pool of DGI at the plasma membrane as determined by the fact that this pool of DGI never became sensitive to extracellular trypsin digestion (Figs. 2 and 3). Second, inhibition of DGI processing in cells treated with tunicamycin in the absence of cell–cell contact blocked DGI transfer into the insoluble pool and transport to the plasma membrane (Fig. 6). These results indicate that the formation of an insoluble pool of DGI must occur intracellularly (see above) and that it is an obligatory step in the transport of DGI to the plasma membrane and the formation of desmosomes.

Regulation of Assembly of the Cytoplasmic Plaque and Membrane Core Domains during Desmosome Formation

This detailed kinetic analysis of DGI biosynthesis taken together with our similar analysis of DPI/II (38, 39, and see the introduction to this article) provide a strong basis for an initial comparison of the stages in assembly of the membrane core and cytoplasmic plaque domains of the desmosome. There are several striking similarities in the biosynthesis of these proteins. First, upon synthesis both DPI/II and DGI initially enter a soluble pool of protein. Detailed analysis of the sedimentation of the soluble pools of these proteins shows that the peak fractions have a similar sedimentation rate of 7.0–7.5 S. However, the distribution of DGI is skewed to the heavy end of the gradient (data not shown), while that of DPI/II is skewed to the light end of the gradient (38). We are at present analyzing the overlapping fractions in more detail to determine whether DPI/II and DGI are part of a complex (see also below). Second, both DPI/II and DGI are titrated into an insoluble pool of protein as defined by the relative extractability of the proteins in CSK buffer (see below). Third, the formation of insoluble pools of these proteins does not require cell–cell contact per se. Fourth, the metabolic stability of both DPI/II and DGI increases ~10-fold upon induction of cell–cell contact.

Although the processing and assembly of DPI/II and DGI appear to be similar, the kinetics are quite different. For instance, a small portion of DPI/II (~20–30%) enters the insoluble pool almost immediately upon synthesis, whereas the insoluble pool of DGI forms ~30–90 min after synthesis. In addition, although cell–cell contact increases the capacity of the insoluble pools of both proteins, the rate of titration is different; <60 min for DGI, and 3–5 h for DPI/II. Taken together these results indicate that initial stages in the assembly of the membrane core and cytoplasmic plaque domains are noncoordinate, but that the formation of the desmosome occurs by the integrated assembly of the two domains at the plasma membrane.

Based upon these results, we propose a simple, testable model of the steps involved in the assembly of these domains. We suggest that initially newly synthesized DGI enters an insoluble pool of protein in the *trans*-Golgi complex. Although we do not yet know how this pool of protein is formed we suggest that insolubility may result from clustering of DGI in the plane of the lipid bilayer, perhaps with other components of the membrane core domain. DGI is then transported in vesicles to the plasma membrane. Concurrently newly synthesized DPI/II and perhaps other components of the cytoplasmic plaque domain are present in the cytoplasm in soluble and insoluble pools that are associated with cytokeratin intermediate filaments (see Fig. 4, reference 39). In the absence of cell–cell contact and desmosome formation the two domains are not induced to coassemble into complexes on the membrane and, as a consequence, remain metabolically unstable and are degraded rapidly.

Induction of cell–cell contact causes a dramatic change in the spatial organization and metabolic fate of the proteins. We suggest that this is initiated by the aggregation of small clusters of DGI and associated proteins on the plasma membrane at the areas of cell–cell contact. This process may be analogous to ligand-induced patching of cell surface receptors and elements of the peripheral cytoskeleton (1, 29). How might this patching be induced? Cowin et al. (5) have shown that components of the membrane core interact functionally on the plasma membranes of adjacent cells; such interactions might trigger the aggregation of membrane core clusters. Alternatively, initial patching may be induced by the cell adhesion molecule, uvomorulin, which appears to initiate

cell-cell adhesion (17) by homotypic interactions of proteins on adjacent cells (28). We suggest that the formation of patches or aggregates of DGI together with other components of the membrane core domain on the plasma membrane may act as a nucleation site for the targeting and assembly on the plasma membrane of components of the cytoplasmic plaque domain (e.g., DPI/II). The increase in the number and affinity of binding sites may increase the capacity of the insoluble pools of protein resulting in an increased efficiency of titration from the soluble to insoluble pools, as shown in our experiments (see Figs. 2 and 3). The formation of an integrated complex of cytoplasmic plaque and membrane core domains results in the increased metabolic stability of the constituent proteins. This type of regulation would ensure not only that desmosome assembly was strictly dependent upon cell-cell contact, but also that assembly was initiated only at discrete and symmetrical sites on the plasma membrane of adjacent cells.

Although we interpret our kinetic analyses to suggest that complexes of DPI/II and DGI are assembled separately before arrival at the plasma membrane, we cannot exclude at present the possibility that a complex that includes both proteins is formed at the time DGI becomes insoluble; such a complex might include, for instance, proteins synthesized at different times. However, we can distinguish between these possibilities by comparing the intracellular distribution of the proteins before cell-cell contact, and by biochemical analysis of the insoluble pools of DPI/II and DGI. The results of these studies will be reported later.

We would like to thank Dr. Karl Matlin (Harvard Medical School) for his advice about the 19°C block, and to Secretarial Services for typing the manuscript.

This work was supported by a Grant-in-Aid from the American Heart Association and with funds contributed in part by the American Heart Association Pennsylvania Affiliate (88-1106) to W. J. Nelson, and in part by grants from the National Institutes of Health (GM 35527) and National Science Foundation (DCB-8609091) to W. J. Nelson, from the National Institutes of Health to the Institute for Cancer Research (CA-06927, RR-05539), and an appropriation from the Commonwealth of Pennsylvania. M. Pasdar was also supported in part by a National Institutes of Health Postdoctoral Fellowship (CA-09035). W. J. Nelson is an Established Investigator of the American Heart Association.

Received for publication 11 November 1988 and in revised form 17 February 1989.

References

1. Bourguignon, L. Y. W., and S. J. Singer. 1977. Transmembrane interactions and mechanisms of capping of surface receptors by their specific ligands. *Proc. Natl. Acad. Sci. USA.* 74:5031-5035.
2. Cohen, S. M., G. Gorbsky, and M. S. Steinberg. 1983. Immunochemical characterization of related families of glycoproteins in desmosomes. *J. Biol. Chem.* 258:2621-2627.
3. Cowin, P., and D. R. Garrod. 1983. Antibodies to epithelial desmosomes show wide tissue and species cross reactivity. *Nature (Lond.).* 302: 148-150.
4. Cowin, P., D. L. Mattey, and D. R. Garrod. 1984. Distribution of desmosomal components in the tissues of vertebrates studied by fluorescent antibody staining. *J. Cell. Sci.* 66:119-132.
5. Cowin, P., D. L. Mattey, and D. R. Garrod. 1984. Identification of desmosomal surface components (desmocollins) and inhibition of desmosome formation by specific Fab. *J. Cell. Sci.* 70:41-60.
6. Cowin, P., W. W. Franke, C. Grund, H. P. Kapperell, and J. Kartenbeck. 1985. The desmosome-intermediate filament complex. *In* The Cell in Contact: Adhesion and Junctions as Morphogenetic Determinants. G. Edelman and J. P. Thiery, editors. John Wiley & Sons, New York. 427-460.
7. Cowin, P., H. P. Kapprell, and W. W. Franke. 1985. The complement of desmosomal plaque proteins in different cell types. *J. Cell. Biol.* 101: 1442-1454.
8. Cowin, P., H. P. Kapprell, W. W. Franke, J. Tamkun, and R. O. Hynes. 1986. Plakoglobin: a protein common to different kinds of intercellular adhering junctions. *Cell.* 46:1063-1073.
9. Czichi, U., and W. J. Lennarz. 1977. Localization of the enzyme system for glycosylation via the lipid-linked pathway in rough endo plasmic reticulum. *J. Biol. Chem.* 252:7901-7904.
10. Drochmans, P., C. Freudenstein, J. C. Wanson, L. Lewrent, T. W. Keenan, J. Stadler, R. Leloup, and W. W. Franke. 1978. Structure and biochemical composition of desmosome and tonofilaments isolated from calf muzzle epidermis. *J. Cell. Biol.* 79:427-443.
11. Dunphy, W. G., R. Brands, and J. E. Rothman. 1985. Attachment of terminal N-acetylglucosamine to asparagine-linked oligosaccharides occurs in central cisternae of the Golgi stack. *Cell.* 40:463-472.
12. Franke, W. W., H. Mueller, S. Mittnacht, H. P. Kapprell, and J. L. Jorcano. 1983. Significance of two desmosome plaque-associated polypeptides of molecular weights 75,000 and 83,000. *EMBO (Eur. Mol. Biol. Organ.) J.* 2:2211-2215.
13. Franke, W. W., E. Schmid, C. Grund, H. Muller, H. Engelbrecht, R. Moll, J. Stadler, and E. D. Jarasch. 1981. Antibodies to high molecular weight polypeptides of desmosome: specific localization of a class of junctional proteins in cells and tissues. *Differentiation.* 20:217-241.
14. Garrod, D. R. 1986. Formation of desmosomes in polarized and nonpolarized epithelial cells: implications for epithelia morphogenesis. *Biochem. Soc. Trans.* 14:172-175.
15. Garrod, D. R., and P. Cowin. 1986. Desmosomes structure and function. *In* Receptors in Tumor Biology. C. M. Chadwick, editor. Cambridge University Press. 95-130.
16. Geiger, B., E. Schmid, and W. W. Franke. 1983. Spatial distribution of proteins specific for desmosomes and adherens junctions in epithelial cells demonstrated by double immunofluorescence microscopy. *Differentiation.* 23:189-205.
17. Gumbiner, B., B. Stevenson, and A. Grimaldi. 1988. The role of the cell adhesion molecule uvomorulin in the formation and maintenance of the epithelial junctional complex. *J. Cell. Biol.* 107:1575-1587.
18. Hubbard, S. C., and R. J. Ivatt. 1981. Synthesis and processing of asparagine-linked oligosaccharides. *Annu. Rev. Biochem.* 50:555-584.
19. Johnson, D. C., and P. G. Spear. 1982. Monensin inhibits the processing of herpes simplex virus glycoproteins, their transport to the cell surface, and the egress of virions from infected cells. *J. Virol.* 43:1102-1112.
20. Kelly, D. E. 1966. Fine structure of desmosomes, hemi-desmosomes and an adepidermal globular layer in developing newt epidermis. *J. Cell. Biol.* 28:51-72.
21. Kelly, D. E., and F. L. Shienvold. 1976. The desmosome: fine structure studies with freeze-fracture replication and tannic acid staining of sectioned epidermis. *Cell Tissue Res.* 172:309-323.
22. Kapprell, H. P., P. Cowin, and W. W. Franke. 1985. Biochemical characterization of desmosomal proteins isolated from bovine muzzle epidermis: amino acid and carbohydrate composition. *Eur. J. Cell. Biol.* 36: 217-229.
23. Lamelli, U. K. 1970. Cleavage of structural proteins during the assembly of the head of bacteriophage T4. *Nature (Lond.).* 227:680-685.
24. Mattey, D. L., and D. R. Garrod. 1986. Calcium-induced desmosome formation in cultured epithelial cells. *J. Cell Sci.* 85:95-111.
25. Matlin, K. S., and K. Simons. 1983. Reduced temperature prevents transfer of a membrane glycoprotein to the cell surface but does not prevent terminal glycosylation. *Cell.* 34:233-243.
26. Miller, K., D. Mattey, H. Measures, C. Hopkins, and D. Garrod. 1987. Localization of the protein and glycoprotein components of bovine nasal epithelial desmosomes by immunoelectron microscopy. *EMBO (Eur. Mol. Biol. Organ.) J.* 6:885-889.
27. Mueller, H., and W. W. Franke. 1983. Biochemical and immunological characterization of Desmoplakins I and II, the major polypeptides of the desmosmal plaque. *J. Mol. Biol.* 163:647-671.
28. Nagafuchi, A., Y. Shirayoshi, K. Okazaki, K. Yasuda, and M. Takeichi. 1987. Transformation of cell adhesion properties by exogenously introduced E-cadherin cDNA. *Nature (Lond.).* 329:341-343.
29. Nelson, W. J., C. A. L. S. Colaco, and E. Lazarides. 1983. Involvement of spectrin in cell-surface receptors capping in lymphocytes. *Proc. Natl. Acad. Sci. USA.* 80:1626-1630.
30. Nelson, W. J., and P. J. Veshnock. 1986. Dynamics of membrane-skeleton (fodrin) organization during development of polarity in Madin-Darby kidney epithelial cells. *J. Cell Biol.* 103:1751-1765.
31. Nelson, W. J., and P. J. Veshnock. 1987. Modulation of membrane-skeleton (fodrin) stability by cell-cell contact in Madin-Darby canine kidney epithelial cells. *J. Cell Biol.* 104:1527-1537.
32. Overton, J. 1962. Desmosome development in normal and reassociating cells of early chick blastoderm. *Dev. Biol.* 4:532-548.
33. Overton, J. 1973. Experimental manipulation of desmosome formation. *J. Cell Biol.* 56:636-646.
34. Overton, J. 1974. Cell junctions and their development. *Prog. Surf. Membr. Sci.* 8:161-208.
35. Overton, J. 1974. Selective formation of desmosomes in chick cell reag-

gregates. *Dev. Biol.* 39:210–225.
36. Overton, J. 1975. Experiments with junctions of the adherens types. *Curr. Top. Dev. Biol.* 10:1–34.
37. Overton, J. 1982. Inhibition of desmosome formation with tunicamycin and with lectin in corneal cell aggregates. *Dev. Biol.* 92:66–72.
38. Pasdar, M., and W. J. Nelson. 1988. Kinetics of desmosome assembly in Madin–Darby canine kidney epithelial cells: temporal and spatial regulation of desmoplakin organization and stabilization upon cell–cell contact. I. Biochemical Analysis. *J. Cell Biol.* 106:677–685.
39. Pasdar, M., and W. J. Nelson. 1988. Kinetics of desmosome assembly in Madin–Darby canine kidney epithelial cells: temporal and spatial regulation of desmoplakin organization and stabilization upon cell–cell contact. II. Morphological analysis. *J. Cell Biol.* 106:687–695.
40. Penn, E. J., C. Hobson, D. A. Rees, and A. I. Magee. 1987. Structure and assembly of desmosome junctions: biosynthesis, processing, and transport of the major protein and glycoprotein components in cultured epithelial cells. *J. Cell Biol.* 105:57–68.
41. Penn, E. J., I. D. J. Burdett, C. Hobson, and A. I. Magee. 1987. Structure and assembly of desmosome junctions: biosynthesis and turnover of the major desmosome components of Madin–Darby canine kidney cells in low calcium medium. *J. Cell Biol.* 105:2327–2334.
42. Rodriguez, J., and F. Deinhardt. 1960. Preparation of semipermanent mounting medium for fluorescent antibody studies. *Virology.* 12:316–317.
43. Singh, U. K., R. K. Maheshwari, G. P. Damewood IV, C. B. Stephensen, C. Oliver, and R. H. Freidmen. 1988. Interferon alters intracellular transport of vesicular stomatitis virus glycoprotein. *J. Biol. Reg. Homeost. Ag.* 2:53–63.
44. Skerrow, C. J. 1985. Desmosomal proteins. *In* Biology of the Integuments. Vol. 2. Vertebrates. J. Bereiter-Hahn, A. G. Matoltsy, and K. S. Richards, editors. Springer-Verlag, Berlin/Heidelberg/New York/Tokyo. 763–787.
45. Skerrow, C. J., I. Hunter, and D. Skerrow. 1987. Dissection of the bovine epidermal desmosome into cytoplasmic protein and membrane glycoprotein. *J. Cell Sci.* 87:411–421.
46. Skerrow, C. J., and A. G. Matoltsy. 1974. Isolation of epidermal desmosomes. *J. Cell Biol.* 63:515–523.
47. Suhrbier, A., and D. Garrod. 1986. An investigation of the molecular components of desmosomes in epithelial cells of five vertebrates. *J. Cell Sci.* 81:223–242.
48. Tarentino, A. L., R. B. Trimble, and F. Maley. 1978. Endo-β-N-acetylglucosaminidase from streptomycesplicatus. *Methods Enzymol.* 50:574–580.
49. Tartakoff, A. M. 1983. Perturbation of vesicular traffic with the carboxylic ionophore monensin. *Cell.* 32:1026–1028.
50. Tartakoff, A. M., and P. Vassalli. 1977. Plasma cell immunoglobulin secretion arrest is accompanied by alterations of the Golgi complex. *J. Exp. Med.* 146:1332–1345.
51. Tkacz, J. S., and J. O. Lampen. 1975. Tunicamycin inhibition of polyisoproline N-acetylglucosaminyl pyrophosphate formation in calf-liver microsome. *Biochem. Biophys. Res. Commun.* 65:248–257.
52. Towbin, H., T. Staehlin, and J. Gordon. 1979. Electrophoretic transfer of proteins from polyacrylamide gels to nitrocellulose sheets: procedures and some applications. *Proc. Natl. Acad. Sci. USA.* 76:4350–4354.